

The Generalization of the Kinetic Equations and the Spectral Conductivity Function to Anisotropic Systems: Case T-Al_{72.5}Mn_{21.5}Fe₆ Complex Metallic Alloy

Popčević, Petar; Batistić, Ivo; Tutiš, Eduard; Velebit, Kristijan; Heggen, Marc; Feuerbacher, Michael

Source / Izvornik: **Croatica Chemica Acta**, 2010, 83, 95 - 100

Journal article, Published version

Rad u časopisu, Objavljena verzija rada (izdavačev PDF)

Permanent link / Trajna poveznica: <https://um.nsk.hr/um:nbn:hr:217:387029>

Rights / Prava: [Attribution 4.0 International](#)/[Imenovanje 4.0 međunarodna](#)

Download date / Datum preuzimanja: **2024-04-17**



Repository / Repozitorij:

[Repository of the Faculty of Science - University of Zagreb](#)



The Generalization of the Kinetic Equations and the Spectral Conductivity Function to Anisotropic Systems: Case T-Al_{72.5}Mn_{21.5}Fe₆ Complex Metallic Alloy*

Petar Popčević,^a Ivo Batistić,^{b,**} Eduard Tutiš,^a Kristijan Velebit,^a Marc Heggen,^c and Michael Feuerbacher^c

^aLaboratory for the Physics of Transport Phenomena, Institute of Physics, Bijenička c. 46, P. O. Box 304, HR-10001 Zagreb, Croatia

^bDepartment of Physics, Faculty of Science, University of Zagreb, Bijenička c. 32, HR-10000 Zagreb, Croatia

^cInstitut für Festkörperforschung, Forschungszentrum Jülich, D-52425 Jülich, Germany

RECEIVED DECEMBER 23, 2009; REVISED JANUARY 19, 2010; ACCEPTED JANUARY 20, 2010

Abstract. Electrical conductivity, σ , and thermoelectric power, S , of the monocrystalline T-Al_{72.5}Mn_{21.5}Fe₆ complex metallic alloy have been investigated in the temperature range from 2 to 300 K. The crystallographic-direction-dependent measurements were performed along the [0 0 1], [0 1 0] and [1 0 0] directions of the orthorhombic unit cell, where the stacking direction is along the [0 1 0] direction. The electrical conductivity exhibits a very small anisotropy, and in all directions shows the non-metallic behaviour with square root, \sqrt{T} , temperature behaviour and finite value in the $T = 0$ limit. Spectral conductivity function, $\sigma_s(E)$, constructed out of measurements, reflects anisotropy of the experimental data and indicate non-analytic square root like singularity at Fermi level. Asymmetry of the spectral conductivity function has been extracted from the thermoelectric power data.

Keywords: spectral conductivity function, anisotropic systems, transport coefficients, complex metallic alloys, Taylor phases

INTRODUCTION

Complex metallic alloys (CMA) are intermetallics phases consisting of two, or more constituent metallic elements but having unusually complex structure. Their unit cells comprise up to several thousand atoms. Within CMA family there exist quasicrystalline phase which can be quasiperiodic in all three spatial direction (icosahedral quasicrystals) or just in two of them (polygonal quasicrystals). The last one expresses periodic stacking of the quasiperiodic planes. Approximant crystalline phases are particularly important for the understanding of the physical properties of the decagonal quasicrystals because of the similarity of the local atomic arrangement. Recently, the anisotropic transport properties measured along three orthogonal crystallographic directions were reported for three decagonal approximant phases of increasing structural complexity comprising two, four and six atomic layers in the unit cell. The first was the Al₇₆Co₂₂Ni₂ compound,^{1,2} which is a monoclinic approximant to the decagonal phase with two atomic layers within one periodic unit of ≈ 0.4 nm along the

stacking direction and a relatively small unit cell, comprising 32 atoms. The second was the orthorhombic o-Al₁₃Co₄ decagonal approximant,^{3,4} which comprises four atomic layers within one periodic unit of ≈ 0.8 nm along the stacking direction and a larger unit cell with 102 atoms. The third, which is approximant to the decagonal phase, was Al₈₀Cr₁₅Fe₅,^{5,6} with six atomic layers in a periodic unit of 1.25 nm and 306 atoms in the giant unit cell. Common to all these phases is large anisotropy of the transport properties between the stacking and in-plane directions, where the crystals show the highest conductivity along the stacking direction (corresponding to the periodic direction in d-QCs). At the same the in-plane anisotropy is considerably smaller, yet significant. In this paper we present anisotropic transport (electrical conductivity and thermopower) properties of the monocrystalline T-Al_{72.5}Mn_{21.5}Fe₆ complex metallic alloy. This is ternary extension of the binary T-Al₇₃Mn₂₂ phase first discovered by Hofman⁷ and later studied by Taylor⁸ thus often referred as Taylor (T) phase. It is closely related to the decagonal quasicrystals. The structure of the Taylor phase can be viewed as stacking of the atomic

* Presented at the EU Workshop "Frontiers in Complex Metallic Alloys", Zagreb, October 2008.

Dedicated to Professor Boran Leontić on the occasion of his 80th birthday.

** Authors to whom correspondence should be addressed. (E-mail: ivo@phy.hr)

layers along the [010] crystallographic direction with ten layers within one unit cell.⁹

In this paper, transport properties of the monocrystalline T-Al_{72.5}Mn_{21.5}Fe₆ complex metallic alloy are analysed within the Kubo Greenwood response theory.^{10–12} The central quantity of this formalism is spectral conductivity function, $\sigma_S(E) = n(E) \cdot D(E)$, where $n(E)$ is the density of states which contains information about the band structure, and $D(E) = \bar{v}(E)^2 \cdot \tau(E)$ is the diffusivity in which transport properties are incorporated through mean square velocity of the particles in the system, $\bar{v}(E)^2$, and the scattering relaxation time $\tau(E)$. In this formalism all temperature dependence of the transport coefficients are introduced through the Fermi-Dirac distribution function, while all peculiarities of the scattering processes are incorporated in the spectral conductivity function through its energy dependence.¹³ In principle, the spectral conductivity function can be calculated theoretically from the band structure calculations and the related scattering processes. Here we use experimental data to determine spectral conductivity function in vicinity of the Fermi level.

EXPERIMENTAL

Electrical conductivity and thermoelectric power of the monocrystal T-Al_{72.5}Mn_{21.5}Fe₆ along all three crystallographic directions were measured. From Czochralski-grown crystal three bar shaped samples (with approximate dimensions $1 \times 1 \times 2.5 \text{ mm}^3$) were cut with their long directions pointing along the three orthogonal crystal axes. The chemical composition was determined by the SEM/EDX. Electrical conductivity, $\sigma(T)$, was measured using the standard four-terminal technique and thermoelectric power, $S(T)$, was measured using a differential method with two identical thermocouples (chromel-gold with the fraction of Fe atoms of 0.07 %), attached to the sample with silver paint.¹⁴ The measurements of the electrical conductivity and thermopower were performed simultaneously from 2 to 300 K in the heating regime.

RESULTS AND DISCUSSION

Electrical conductivity for the three different crystallographic directions of the monocrystalline T-Al_{72.5}Mn_{21.5}Fe₆ exhibits a non-metallic behaviour in the whole measured temperature range (Figure 1). A small anisotropy amounting to 1.14 and 1.12 can be observed between in plane ([001] and [100]) and stacking [010] directions, respectively. Electrical conductivity is the highest in the stacking direction amounting to $2270 \text{ } \Omega^{-1} \text{ cm}^{-1}$ on room temperature. In inplane [001] and [100] directions, the electrical conductivities are $2000 \text{ } \Omega^{-1} \text{ cm}^{-1}$ and $2020 \text{ } \Omega^{-1} \text{ cm}^{-1}$, respectively, showing almost negligibly anisotropy (≈ 1.01). This is in

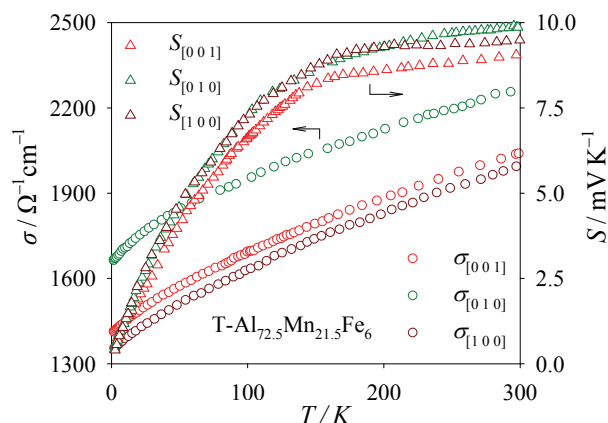


Figure 1. The electrical conductivity, $200\sigma(T)$, and the thermopower, $S(T)$, for the three different crystallographic directions of the monocrystalline T-Al_{72.5}Mn_{21.5}Fe₆ versus temperature, T .

accordance with previous measurements of the decagonal approximant phases which shows decrease in anisotropy with increasing number of stacking planes in the one periodic unit.^{1,3,5}

Temperature dependence of the electrical conductivity, $\sigma(T)$, shows similar \sqrt{T} behaviour as observed on polycrystalline T-AlMn(Fe,Pd) complex metallic alloys^{17,18} and polycrystalline decagonal quasicrystal d-Al₇₃Mn₂₁Fe₆.¹⁷ Similar behaviour has been reported in other quasicrystal compound.^{19,20} In general, a very good fit to experimental data can be obtained by using the following formula:

$$\sigma(T) = \sigma_0 + \sigma_1 \sqrt{T} + \sigma_2 T \quad (1)$$

The corresponding fits to our experimental data are shown in Figure 2 as full lines. The absolute value of the electrical conductivity of the here presented monocrystalline T-Al_{72.5}Mn_{21.5}Fe₆ is almost two times larger than that of the polycrystalline d-Al₇₃Mn₂₁Fe₆.¹⁷

The experimental data of thermoelectric power of the T-Al_{72.5}Mn_{21.5}Fe₆ in three crystallographic directions are shown in Figure 1. The positive $S(T)$ values indicate that holes are the dominant charge carriers. The room temperature value amounts to $9.5 \text{ } \mu\text{V K}^{-1}$ which is in accordance with previously²¹ observed increase of the thermoelectric power with increasing Fe fraction substituted in the binary T-Al₇₃Mn₂₇ alloy. A negligible anisotropy is observed between in plane thermoelectric powers $S_{[001]}$ and $S_{[100]}$. The thermopower in the third direction [010] exhibits something different high temperature increase.

Modeling

In an isotropic material the electrical conductivity, thermoelectric power (Seebeck coefficient) and electron

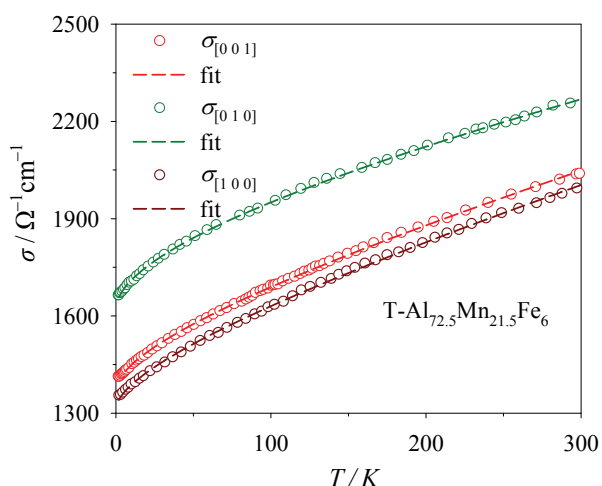


Figure 2. The electrical conductivity, $\sigma(T)$, for the three different crystallographic directions of the monocrystalline T-Al_{72.5}Mn_{21.5}Fe₆ versus temperature, T . The circles represent the experimental data. The full line represents the fit to Eq. (1).

thermal conductivity, $\kappa(T)$, can be expressed¹² in terms of kinetic coefficients L_{ij} :

$$\begin{aligned}\sigma(T) &= L_{11}(T) \\ S(T) &= \frac{1}{eT} \frac{L_{12}(T)}{\sigma(T)} \\ \kappa(T) &= \frac{1}{e^2 T} L_{22}(T) - T \cdot \sigma(T) \cdot S(T)^2,\end{aligned}\quad (2)$$

where the kinetic coefficients are related to the spectral conductivity as:

$$L_{\alpha\beta}(T) = (-1)^{\alpha+\beta} \int dE \sigma_s(E) \cdot (E - \mu)^{\alpha+\beta-2} \times \left(-\frac{\partial f(E, \mu, T)}{\partial E} \right) \quad (3)$$

and $f(E, \mu, T)$ is the Fermi-Dirac distribution function and $\mu(T)$ is the chemical potential. In an anisotropic material, the kinetic coefficients, L_{ij} will be tensors. The transport equations

$$\begin{aligned}J_i &= \sum_j L_{11,ij} \left(E_j + T \frac{\partial \mu}{\partial x_j} \frac{1}{T} \right) + \sum_j L_{12,ij} \frac{\partial T}{\partial x_j} \\ Q_i &= \sum_j L_{21,ij} \left(E_j + T \frac{\partial \mu}{\partial x_j} \frac{1}{T} \right) + \sum_j L_{22,ij} \frac{\partial T}{\partial x_j}\end{aligned}\quad (4)$$

where $\vec{J} = (J_x, J_y, J_z)$ is the electrical current, $\vec{Q} = (Q_x, Q_y, Q_z)$ is the heat current, and $\vec{x} = (x, y, z)$, contain 21 transport coefficients. With a special selection of the coordinate axes one may reduce this 21 to 18 independent transport coefficients. For a general anisotropic

material it is an impossible task to determine all these numbers experimentally.

Fortunately, material studied, possess an orthorhombic symmetry. With appropriate choice of the crystal orientation the transport coefficients for each direction can be measured independently from others. In the system of the principal axes of the medium, the tensors $L_{\alpha,\beta,i,j}$ become diagonal:

$$L_{\alpha,\beta,i,j} = 0 \quad \text{unless } i = j.$$

The usual procedure^{8,11} in determination of the spectral conductivity function from the experimental data can be applied for each direction separately. The transport properties are characterized with three spectral conductivity functions, one for each direction:

$$L_{\alpha,\beta,ij}(T) = (-1)^{\alpha+\beta} \int dE \sigma_{s,i}(E) \cdot (E - \mu)^{\alpha+\beta-2} \times \left(-\frac{\partial f(E, \mu, T)}{\partial E} \right) \quad (5)$$

The temperature dependence of the thermoelectric power and electrical conductivity comes from the Fermi-Dirac function explicitly while implicit temperature dependence through the chemical potential is neglected. The temperature dependence of the chemical potential is regularly derived through the Sommerfeld expansion and it leads to the T^2 (and higher powers of T) behaviour. In our case T^2 and higher order are negligible small suggesting that we should neglect the temperature dependence of the chemical potential. In addition the Sommerfeld expansion doesn't apply in the case of the singular behaviour near the Fermi surface as is here.

The approximation of the temperature independence of the chemical potential allows us to divide spectral conductivity function to symmetric and antisymmetric part, and separately calculate firstly symmetric part which is entirely determined by the electrical conductivity data, and then antisymmetric part which is determined by the product of the thermoelectric power and the electrical conductivity. The whole spectral conductivity function thus can be written in the form:

$$\sigma_{s,i}(E) = \sigma_{s,i}^s(E) + \sigma_{s,i}^a(E)$$

where:

$$\sigma_{s,i}^s(E) = \frac{1}{2} \cdot (\sigma_{s,i}(E) + \sigma_{s,i}(-E))$$

$$\sigma_{s,i}^a(E) = \frac{1}{2} \cdot (\sigma_{s,i}(E) - \sigma_{s,i}(-E))$$

From the temperature dependence of the electrical conductivity data in Eq.(1) and using Eqs.(2) and (5) we deduce functional form of:

$$\sigma_{s,i}^s(E) = \sigma_{0,i} + a_i \cdot \sqrt{|E|} + b_i \cdot |E| \quad (6)$$

where coefficients a_i and b_i are related to the parameters $\sigma_{1,i}$ and $\sigma_{2,i}$ with relations obtained through numerical integration of the Eq. (3):

$$a_i = \sigma_{1,i} \cdot 101 \text{ K}^{1/2}$$

$$b_i = \sigma_{2,i} \cdot 8.34 \cdot 10^3 \text{ K}.$$

For the antisymmetric part of the spectral conductivity function we use piecewise linear function (PLF) instead of the polynomial representation. PLF approach seems more practical and physically transparent, since, every abrupt change in slope of $\sigma_{s,i}^a(E)$ is directly related to the some temperature at which the change in the temperature behavior of the thermopower takes place. In the case of the T-Al_{72.5}Mn_{21.5}Fe₆ satisfactory fit is obtained (Figure 3) with two characteristic energies, and

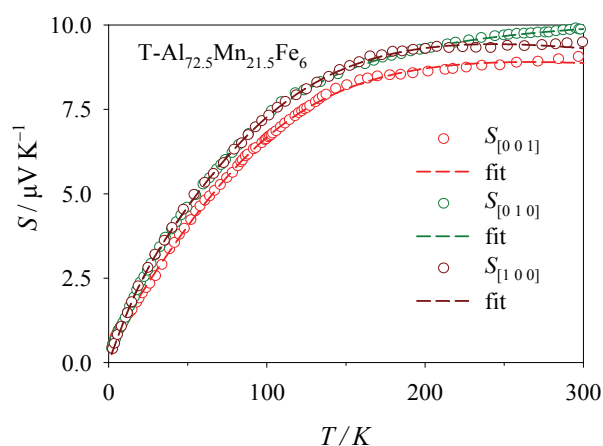


Figure 3. Thermoelectric power, $S(T)$, versus temperature T for the three different crystallographic directions of the monocrystalline T-Al_{72.5}Mn_{21.5}Fe₆. The experimental data are represented by circles. The full line is the result of the spectral conductivity modeling, as presented in the text.

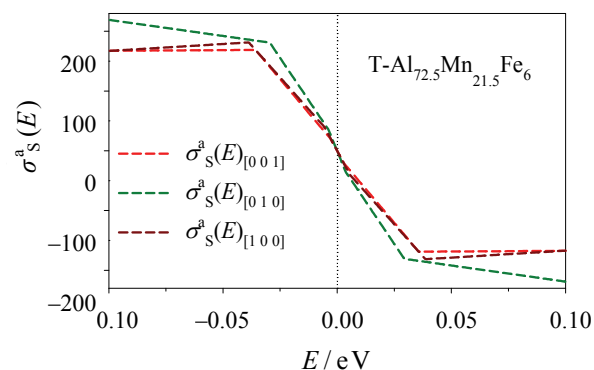


Figure 4. The antisymmetric part of spectral conductivity for the three different crystallographic directions of the monocrystalline T-Al_{72.5}Mn_{21.5}Fe₆. The advantage of this parameterization is direct interpretation of the model parameters as the widths of the characteristic windows in energy with characteristic values of $\sigma_{s,i}^a(E)$ within these windows.

antisymmetric part of the spectral conductivity is then written as:

$$\sigma_{s,i}^a(E) = \begin{cases} c_i \cdot E & \text{for } |E| \leq e_{1,i} \\ d_i \cdot E + [e_{1,i}(c_i - d_i)] & \text{for } e_{1,i} \leq E \leq e_{2,i} \\ f_i \cdot E + [e_{1,i}(c_i - d_i) + e_{2,i}(d_i - f_i)] & \text{for } e_{2,i} \leq E \\ -\sigma_{s,i}^a(-E) & \text{for } E \leq 0 \end{cases}$$

The resulting fits of $\sigma_{s,i}^a(E)$ are shown in Figure 4. Due to negligible small anisotropy of the $S(T)$ data anisotropy of the $\sigma_{s,i}^a(E)$ are too small. Minute deviation of the $\sigma_{s,i}^a(E)_{[010]}$ is consequence of the high temperature increase of the thermoelectric power data

Characteristic energies at which abrupt changes in $\sigma_{s,i}^a(E)$ take place as well as full set of parameters that parameterize the spectral conductivity function are shown in Table 1. Energy e_2 is connected to the change in slope that appear around 150 K in the thermoelectric power data while energy e_1 takes care of the slightly concaveness of the $S(T)$ below 150 K. It can be seen in the Table 1 that the anisotropy is the most pronounced between [0 1 0] direction on one side and two in plane

Table 2. The fitting parameters of the spectral conductivity function for the three different crystallographic directions of the monocrystalline T-Al_{72.5}Mn_{21.5}Fe₆. The parameters σ_0 , a , b , c , d and f share the same unit, $\Omega^{-1} \text{ cm}^{-1}$, whereas e_1 and e_2 are expressed in eV

| Crystal direction | symmetric part | | | asymmetric part | | | | |
|-------------------|----------------|------|------|-----------------|-------|-------|-------|------|
| | σ_0 | a | b | c | e_1 | d | e_2 | f |
| [0 0 1] | 1369 | 2225 | 8232 | -6910 | 0.003 | -4525 | 0.036 | 22 |
| [0 1 0] | 1618 | 2744 | 4939 | -9298 | 0.004 | -5673 | 0.029 | -540 |
| [1 0 0] | 1309 | 2124 | 9151 | -7192 | 0.006 | -4274 | 0.039 | 232 |

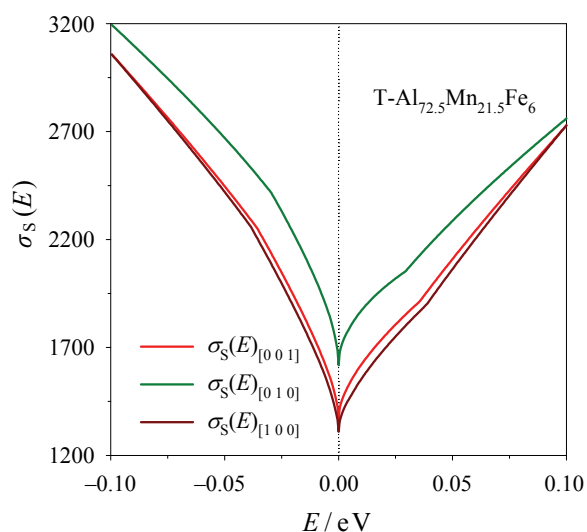


Figure 5. The spectral conductivity, $\sigma_{S,i}^a(E)$, for the three different crystallographic directions of the monocrystalline T-Al_{72.5}Mn_{21.5}Fe₆. The singularities around the Fermi energy ($E = 0$) are clearly pronounced. The sharpness of the pseudogap is directly related to the convex behavior of the electric conductivity $\sigma(T)$ at low temperatures. The symmetric part, clearly dominates the spectral conductivity function.

directions on another side as shown in Figure 5. In $[0 1 0]$ direction the square root term is the most pronounced while linear term is almost two times smaller than in the in plane directions. The mentioned crystal direction possesses the most asymmetric spectral conductivity function which is the direct consequence of the increase of the $S(T)$ in that direction in comparison with the in plane directions.

Our analysis based on the transport measurements carried out from 2 to 300 K revealed fine structure of the pseudogap which shows $\sqrt{|E|}$ singularity at the Fermi level. Similar singularities have been observed in several quasicrystals through low temperature tunneling experiments,²² and theoretically predicted.²³⁻²⁵

CONCLUSION

From the measurements of electrical conductivity and thermoelectric power on monocrystalline T-Al_{72.5}Mn_{21.5}Fe₆ spectral conductivity function has been extracted for all three crystal directions. It shows near square root singularity at Fermi level as suggested from electrical conductivity data. To examine this singularity in more detail it is necessary to perform electrical conductivity measurements at very low temperatures (below 2 K). Anisotropy observed between stacking and in plane electrical conductivity data is reflected in spectral conductivity function. Temperature behaviour of the thermoelectric power leads to asymmetry in the spectral conductivity function.

Measurements presented here demonstrate importance of the periodicity of the structure, and how transport properties change from regular crystals to quasicrystals. In the case of the here presented monocrystalline T-Al_{72.5}Mn_{21.5}Fe₆ and decagonal quasicrystal d-Al₇₃-Mn₂₁Fe₆¹⁰ the most affected is thermoelectric power that completely changes temperature behavior and is much smaller in the case of d-Al₇₃Mn₂₁Fe₆. The electrical conductivity of the quasicrystal d-Al₇₃Mn₂₁Fe₆ is almost two times smaller than that presented here, but with very similar temperature dependence, so the origin of the difference in value could be monocrystallinity of the sample studied here as opposed to polyquasicrystallinity of the d-Al₇₃Mn₂₁Fe₆ sample.

Acknowledgements. This work was done within the activities of the 6th Framework EU Network of Excellence “Complex Metallic Alloys” (Contract No. NMP3-CT-2005-500140), and has been supported in part by the Ministry of Science, Education and Sports of the Republic of Croatia through the Research Projects: 035-0352826-2848, 035-0352826-2847 and 119-1191458-0512. We thank A. Smontara for helpful discussion.

REFERENCES

1. A. Smontara, I. Smiljanić, J. Ivkov, D. Stanić, O. S. Barišić, Z. Jagličić, P. Gille, M. Komelj, P. Jeglič, M. Bobnar, and J. Dolinšek, *Phys. Rev. B* **78** (2008) 104204-1–104204-13.
2. M. Komelj, J. Ivkov, A. Smontara, P. Gille, P. Jeglič, and J. Dolinšek, *Solid State Commun.* **149** (2009) 515–518.
3. J. Dolinšek, M. Komelj, P. Jeglič, S. Vrtnik, D. Stanić, P. Popčević, J. Ivkov, A. Smontara, Z. Jagličić, P. Gille, and Yu. Grin, *Phys. Rev. B* **79** (2009) 184201-1–184201-12.
4. A. Smontara, D. Stanić, I. Smiljanić, J. Dolinšek, and P. Gille, *Z. Kristallogr.* **224** (2009) 56–58.
5. J. Dolinšek, P. Jeglič, M. Komelj, S. Vrtnik, A. Smontara, I. Smiljanić, A. Bilušić, J. Ivkov, D. Stanić, E. S. Zijlstra, B. Bauer, and P. Gille, *Phys. Rev. B* **76** (2007) 174207-1–174207-13.
6. J. Dolinšek, S. Vrtnik, A. Smontara, M. Jagodić, Z. Jagličić, B. Bauer, and P. Gille, *Philos. Mag.* **88** (2008) 2145–2153.
7. W. Hofmann, *Aluminium* **20** (1938) 865–872.
8. M. A. Taylor, *Acta Metall.* **8** (1960) 256–262.
9. N. C. Shi, X. Z. Li, Z. S. Ma, and K. H. Kuo, *Acta Crystallogr. B* **50** (1994) 22–30.
10. R. Kubo, *J. Phys. Soc. Jpn.* **12** (1957) 570–586.
11. D. A. Greenwood, *Proc. Phys. Soc.* **71** (1958) 585–596.
12. G. V. Chester and A. Thellung, *Proc. Phys. Soc.* **77** (1961) 1005–1013.
13. I. Batistić, D. Stanić, E. Tutiš, and A. Smontara, *Croat. Chem. Acta* **83** (2010) 43–47.
14. A. Smontara, K. Biljaković, J. Mazuer, P. Monceau, and F. Levy, *J. Phys.: Condens. Matter* **4** (1992) 3273–3281.
15. A. Smontara, I. Smiljanić, A. Bilušić, Z. Jagličić, M. Klanjšek, S. Roitsch, J. Dolinšek, and M. Feuerbacher, *J. Alloys Compd.* **430** (2007) 29–38.
16. D. Stanić, P. Popčević, I. Smiljanić, Ž. Bihar, A. Bilušić, I. Batistić, J. Ivkov, A. Smontara, M. Heggen, and M. Feuerbacher, *Croat. Chem. Acta* **83** (2010) 81–86.
17. D. Stanić, P. Popčević, I. Smiljanić, Ž. Bihar, J. Lukatela, B. Leontić, A. Bilušić, I. Batistić, and A. Smontara, *Materiali in tehnologije* **44** (2010) 3–7.

18. D. Stanić, P. Popčević, I. Smiljanić, A. Bilušić, I. Batistić, J. Ivkov, and A. Smontara, *J. Phys.: Conf. Ser.* (2010) in press.
19. N. P. Lalla, R. S. Tiwari, and O. N. Srivastava, *J. Phys.: Condens. Matter* **7** (1995) 2409–2420.
20. P. Volkov and S. J. Poon, *Phys. Rev. B* **52** (1995) 12685–12689.
21. D. Stanić, *Thesis*, Physical Department, University of Zagreb (2009).
22. R. Escudero, J. C. Lasjaunias, Y. Calvayrac, and M. Boudard, *J. Phys.: Condens. Matter* **11** (1999) 383–404.
23. C. V. Landauro, E. Maciá, and H. Solbrig, *Phys. Rev. B* **67** (2003) 184206-1–184206-7.
24. C. Janot, *Phys. Rev. B* **53** (1996) 181–191.
25. C. Janot, *J. Phys.: Condensed Matter* **9** (1997) 1493–1508.

SAŽETAK

Poopćenje kinetičkih jednadžbi i spektralna funkcija za anizotropne sisteme: primjer kompleksne metalne legure $T\text{-Al}_{72.5}\text{Mn}_{21.5}\text{Fe}_6$

Petar Popčević,^a Ivo Batistić,^b Eduard Tutiš,^a Kristijan Velebit,^a Marc Heggen^c i Michael Feuerbacher^c

^aLaboratorij za fiziku transportnih svojstava, Institut za fiziku, Bijenička c. 46, P. P. 304, HR-10001 Zagreb, Hrvatska

^bFizički odsjek, Prirodoslovno-matematički fakultet, Bijenička c. 32, HR-10000 Zagreb, Hrvatska

^cInstitut für Festkörperforschung, Forschungszentrum Jülich, D-52425 Jülich, Germany

Proučavana su transportna svojstva (električna vodljivost i termostruja) monokristala kompleksne metalne legure $T\text{-Al}_{72.5}\text{Mn}_{21.5}\text{Fe}_6$ duž sva tri kristalna smjera u temperaturnom rasponu od 2 do 300 K. Električna vodljivost pokazuje pozitivan temperaturni koeficijent što je temperaturno ponašanje neobično za metale, no s konačnom vrijednosti u niskotemperaturnoj granici $T = 0$ K. Funkcija spektralne vodljivosti konstruirana na temelju izmjerenih podataka posjeduje anizotropiju kao i eksperimentalni podaci, te ukazuje na neanalitički korijenski singularitet na Fermijevom nivou. Za asimetriju funkcije spektralne vodljivosti odgovorna je termostruja.